Landslide basal friction as measured by seismic waves

Emily E. Brodsky
Department of Earth and Space Sciences, University of California, Los Angeles, USA

Evgenii Gordeev
Geophys. Survey of Russ. Acad. of Sci., Petropavlovsk-Kamchatsky, Russia

Hiroo Kanamori
Seismo Lab, California Institute of Technology, USA

Received 23 August 2003; revised 14 October 2003; accepted 21 October 2003; published 16 December 2003.

[1] Dynamical predictions of landslide runout require measurements of the basal friction. Here we present the first seismically determined bounds on the frictional coefficients for three large volcanic landslides. The three landslides (Bezymianny, Russia 1956, Sheveluch, Russia 1964 and Mount St. Helens, USA 1980) have masses that vary by a factor of 5 and were all followed immediately by eruptions. We use teleseismic and regional seismic data to show that all three landslides are consistent with an apparent coefficient of friction of 0.2 which corresponds to an actual areally-averaged frictional coefficient of 0.2–0.6. The apparent friction is independent of the quantity of hot gas subsequently released. *INDEX TERMS:* 7209 Seismology: Earthquake dynamics and mechanics; 7280 Seismology: Volcano seismology (8419); 8419 Volcanology: Eruption monitoring (7280). **Citation:** Brodsky, E. E., E. Gordeev, and H. Kanamori, Landslide basal friction as measured by seismic waves, *Geophys. Res. Lett.*, *30*(24), 2236, doi:10.1029/2003GL018485, 2003.

1. Introduction

[2] The long runout of large landslides, and therefore apparently low basal friction, has long been a subject of intense debate [e.g., *Hsu*, 1975; *Kilburn and Sorensen*, 1998]. Volcanic landslides have even longer runouts relative to their size than other landslides, perhaps due to the importance of hot gas as a driving force or lubricant [*Voight et al.*, 1983; *Siebert*, 1984]. We use seismic data to determine bounds on the basal friction and present the first quantitative comparison of instrumentally measured friction for large, long runout landslides associated with eruptions. The landslide basal force can be measured from the seismic waves radiated by the slide [*Kanamori and Given*, 1982; *Hasegawa and Kanamori*, 1987; *Kawakatsu*, 1994]. Here we use a strictly forward-modeling approach because there are too few historical records to justify an inversion procedure. After discussing the physics of landslides as seismic sources, we show that the historical teleseismic data for the 1964 Sheveluch landslide is consistent with the same apparent coefficient of friction as inferred for the better-recorded and previously well-studied 1980 Mount St. Helens landslide. We then use regional records to demonstrate that the 1956 Bezymianny landslide is consistent with the same apparent friction as the others.

0094-8276/03/2003GL018485

2. Landslides as Seismic Sources

[3] A landslide generates seismic waves by both shearing and loading the surface as the mass moves from a steep to a shallow slope. The effective force system is a horizontal single force [*Kanamori and Given*, 1982; *Dahlen*, 1993]. The amplitude of the seismic waves is proportional to the force drop during the landslide, just as during an earthquake the seismic wave amplitude is proportional to the seismic moment, i.e., the force drop multiplied by the source dimension. For landslides we know an additional variable that is unknown for the earthquake case. We know the gravitational driving force of the landslide while the magnitude of the tectonic forces that drive earthquakes are generally unknown. Therefore, we can find the absolute value of the frictional force for landslides whereas we are unable to perform this calculation for earthquakes.

[4] The shear force between the landslide and the ground is $\mu Mg \cos\theta$ where μ is the dynamic coefficient of friction, M is the mass, g is the gravitational acceleration and θ is the slope angle. As used here, μ and θ are averaged over the entire base of the landslide during motion. By definition, μ is the ratio of the shear force to the normal force.

[5] Assuming that prior to motion the landslide is in static equilibrium, the horizontal component of the force drop on the ground during the landslide during motion is

$$\Delta F_x = Mg(\mu \cos\theta - \sin\theta)\cos\theta. \quad (1)$$

where positive x is the direction of landslide motion. The amplitude of the y-component of the source is predicted to be $\leq$20% of the x-component and is not observed. Irregularities of the slope generate higher frequency perturbations on the signal that can be filtered out of the record. As discussed by *Julian et al.* [1998], the torque associated with displacing a mass a distance L can also generate waves. We modelled the torque as a dipole source to find that the amplitude of the Love waves from the gravitational torque are negligible and the Rayleigh waves are <30% of the amplitude of the waves from the landslide shear.

[6] Equation 1 suggests that as the slope decreases away from the landslide headwall, the horizontal force drop, which is modeled as a single force, gradually increases.

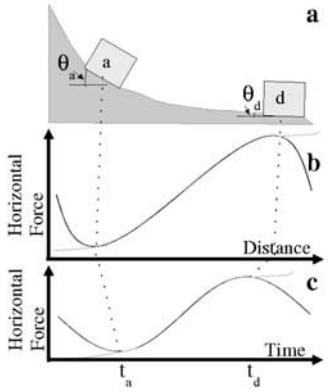

Figure 1. Cartoon of landslide and schematic of force evolution with distance and time. (a) Cartoon of landslide block at two different times. Position a is on a steep slope and corresponds to the peak of the acceleration in panel b. The slope angle here is θ_a. Position d is picked to be the place of maximum deceleration with the slope labeled as θ_d. (b) Schematic of ΔF_x as a function of distance that the block has slid. The grey ends show the predicted source-time function in the absence of the taper caused by the complicating processes discussed in the text. (c) Schematic of ΔF_x as a function of time. The time of the peak acceleration t_a and peak deceleration t_d are labeled. Grey lines are the same as in (b). The dotted lines connect corresponding points on all three panels.

The value of ΔF_x should begin negative, increase through zero and approach μMg on very shallow slopes (Figure 1). This simplified model of the source-time function can be complicated by potentially significant effects such as time-dependent dynamic friction, variable slopes over the extensive basal area of the slide and varying mass of the landslide as retrogressive failure, entrainment and deposition progress.

[7] We deal with these complications empirically by using an observed source-time function as the basis for our interpretations. *Kanamori et al.* [1984] determined the source-time function for the Mount St. Helens landslide by deconvolving the impulse response for a horizontal single force from the observed record. They found that the data is consistent with a sinusoidal source with an amplitude of F_p such as

$$\Delta F_x(t) = -F_p \sin 2\pi t/\tau \qquad 0 \le t < \tau \tag{2}$$

where the duration τ = 240 s for Mount St. Helens. The history of the force drop is similar to that inferred from Equation 1, but the beginning and end of the function taper to 0, probably due to some of the complications mentioned above. An untapered source-time function does not match the timing of the observed surface waves. Incorporating the taper inherent in the source-time function of Equation 2 provides an empirical correction for the complicated time-varying properties and non-rigid body dynamics.

[8] The source-time function in Equation 2 only accounts for the very long-period behavior of the landslide. Higher frequency perturbations caused by bumps and turns in the landslide path do not affect the very long period radiation. In order to capture the overall frictional properties, we attempt to match the longest period sources observable. Modern scanning and digitization technology makes measuring long-period waves on historic paper records feasible. We can now digitally remove the instrument response without overwhelming the signal with noise over a much larger passband than previously possible. We successfully recovered usable signal over the 20–50 s passband for a Russian station with an 11 s corner frequency and signal over the 20–240 s passband for a Benioff 1–90 seismometer.

[9] We call the combination of observables F_p/Mg the apparent coefficient of friction, i.e., $\mu_{app} \equiv F_p/Mg$. If we knew either the slope during the peak of acceleration θ_a or the slope during the peak of deceleration θ_d, then we could use Equations 1–2 to solve for μ given an observed value of μ_{app} (Figure 1). In the absence of an accurate dynamic model for all three landslides studied here, we can only provide bounds on a range of possible slopes θ_a and θ_d, rather than precise values. Therefore, we can only give upper and lower bounds on μ based on our observations of μ_{app}. The slope during deceleration is easier to constrain than during acceleration. If we assume conservatively that at the time of the peak of the deceleration, the bulk of the mass is beyond 1/3 of the final runout distance, then θ_d is small ($\le 20°$) for all three landslides considered here [*Glicken*, 1996; *Belousov*, 1995, 1996]. Therefore, 20° is taken as the maximum of θ_d which we call θ_d^{max}. The minimum value of θ is based on the fact that the average slope over the base is on balance positive for descending landslides, i.e., $\theta \ge 0$. Using these bounds on θ_d and Equations 1–2, we find bounds on μ in terms of μ_{app},

$$\frac{\mu_{app}}{\cos^2 \theta_d^{max}} + \tan \theta_d^{max} \ge \mu \ge \mu_{app} \tag{3}$$

where θ_d^{max} = 20°. The right-hand side of equation 3 is a simplification of $\frac{\mu_{app}}{\cos^2 \theta_d^{min}} + \tan \theta_d^{min}$ where $\theta_d^{min} = 0$. For the specific case of μ_{app} = 0.2, Equation 3 implies that $0.6 \ge \mu \ge 0.2$.

3. Teleseismic Records

[10] Figure 2 shows teleseismic records at comparable distances from the three landslides. We do not attempt to invert the historical data for the source given the limited number and variable quality of the records available. Because of the data limitations, the strategy adopted by this study is to test the hypothesis of a constant value of μ_{app} for consistency with the data. Since the Mount St. Helens seismic source is very well-constrained by data beyond that shown here [*Kanamori and Given*, 1982; *Kanamori et al.*, 1984], we use the amplitude of this landslide force drop as a starting point. We calculated the value of μ_{app} for Mount St. Helens using the *Kanamori et al.* [1984] result and the geological data in Table 1. We then test whether or not the other two landslides are consistent with the same value of μ_{app}. Synthetic surface waves are calculated using a normal mode code complete to l = 1000 with a basic radial mantle model [*Press*, 1970; *Kanamori*, 1970] and the seismic source modeled as a horizontal force in the direction of the landslide runout. The runout directions are constrained by geological maps of the landslides [*Glicken*, 1996; *Belousov*, 1988, 1995]. We only measure the average sliding in the

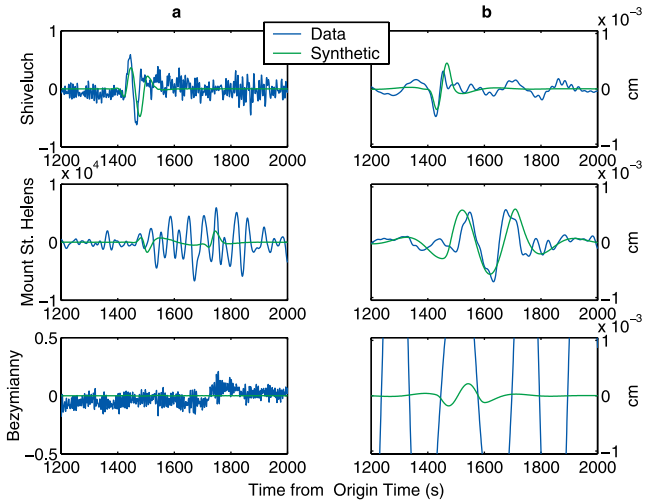

Figure 2. Transverse component of seismic records at epicentral distance $\Delta = 57°-59°$. Bezymianny was recorded on a 1–90 Benioff seismometer in Pasadena, CA; Sheveluch was recorded on a Press-Ewing 30–90 in Pasadena, CA; Mount St. Helens is a digital record from SRO station BOC in Bogota, Colombia. The analog records were digitized from scanned images. (a) The left-hand column are the raw records. (b) The right-hand column are the same records with the instrument response deconvolved over the 20–240 s passband. The spurious long-period oscillations in the Sheveluch record from 1600–2000 s are due to deconvolving a noisy record over a broad bandpass. The Bezymianny deconvolved record shows only noise.

original direction, therefore the duration of our signal for Mount St. Helens is shorter than model-derived times that include the continued flow after a turn into the Toutle River valley [*Voight et al.*, 1983]. The initiation times (origin times) are independently constrained by eyewitness reports, regional and global short-period networks [*Voight*, 1981; *Passechnik*; International Seismological Centre, http://www.isc.ac.uk/bull, 2001]. We use the same functional form for source history from Equation 2 for all the cases in order to limit the number of independent parameters. The only parameter that varies between eruptions is the duration τ.

[11] Figure 2 shows that the Mount St. Helens data is well-matched by the synthetics. This first observation is merely a test of the synthetic method since the assumed value of μ_{app} is based on the well-constrained Mount St. Helens eruption force [*Kanamori and Given*, 1982; *Kanamori et al.*, 1984]. The peak-to-peak amplitude of the synthetic transverse component is 10% less than that of the observed waveform, therefore we conclude that we are unable to resolve amplitude differences of less than 10%. The limit on resolution most likely arises because of errors in the landslide mass, assumed source-time function and source geometry.

[12] More interestingly, Figure 2 also shows that the Sheveluch teleseismic data is well-matched using the same μ_{app} as for Mount St. Helens. A shorter duration source with $\tau = 70$ s was necessary to fit this data. The general agreement in waveform and amplitude suggests that the frictional properties of Sheveluch are similar to Mount St. Helens. The peak-to-peak amplitude of the synthetic is within 4% of the observed signal, i.e., the data and synethic are consistent to within the resolution of the method for $\mu_{app} = 0.2$.

[13] Nothing can be learned from the Bezymianny teleseismic record as noise overwhelms signal at long-periods on this historic instrument.

4. Regional Records

[14] Since the teleseismic records provide no constraints on the Bezymianny landslide, we turn to the regional stations operating in 1956. The most useful of these is the closest station, which is Petropavlovsk (PET) located at 3.16° from the eruption.

[15] The event in the regional records is not an ordinary earthquake. The Bezymianny record Love wave has twice as long a period (30 s rather than 15 s) as would be associated with an ordinary earthquake of this magnitude. Since the origin time of this long-period source is coincident with the beginning of the eruption [*Passechnik*, 1958], the seismogram likely reflects the uncapping landslide and subsequent blast.

Table 1. Comparison of Mount St. Helens, Sheveluch and Bezymianny Volcanic Landslides

	Mount St. Helens 05/18/1980	Sheveluch 11/12/1964	Bezymianny 3/30/1956
Geological observations			
Landslide volume	2.5 km^3[a]	1.2 km^3[b]	0.5 km^3[c]
Landslide mass[d]	5.8×10^{12} kg	2.8×10^{12} kg	1.2×10^{12} kg
Weight[e]	5.7×10^{13} N	2.7×10^{13} N	1.2×10^{13} N
Model Parameters			
μ_{app}	0.2		
τ	240 s	70 s	240 s
Predicted Seismological Observable			
Peak landslide force drop F_p	1×10^{13} N[f]	5×10^{12} N	2×10^{12} N

The value of μ_{app} is based on the well-instrumented Mount St. Helens eruption as explained in the text. The predictions for Sheveluch and Bezymianny are tested in Figures 2 and 3, respectively.

[a] *Glicken* [1996].
[b] *Belousov* [1995].
[c] *Belousov* [1988].
[d] Assumed average density = 2300 kg/m^3.
[e] Weight is *Mg*.
[f] Consistent with *Kanamori et al.* [1984].

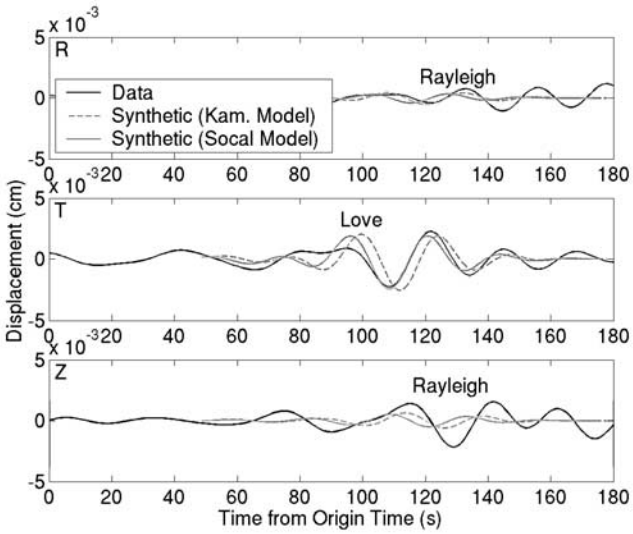

Figure 3. Regional recording of Bezymianny eruption at Petropavlovsk (Δ = 3.16°). Radial (R), transverse (T) and vertical components (Z) are shown with the instrument response is deconvolved over the 20–50 s passband. Time 0 is the origin time (initiation time) of the landslide determined by the entire regional network at the time of the event Passechnik. The Rayleigh wave labeled on the R & Z components is too late to be associated with the labeled Love wave source. Therefore, they are probably due to the blast phase of the eruption as seen for Mount St. Helens [*Kanamori et al.*, 1984] and unrelated to the landslide.

[16] The landslide uncapping the hot magma was the first event in the Bezymianny eruption, therefore it should generate the first waves observed on the seismic record. In Figure 3, we match the Petropavlovsk record with synthetics generated using a discrete wavenumber Green's function program [*Zhu and Rivera*, 2002] with the parameters in Table 1 and two different crustal models. One crustal model is the well-determined, general crustal model determined for Southern California [*Dreger and Helmberger*, 1993] and the other is a less well-constrained, but more locally relevant Kamchatkan model based on a combination of the surface wave and receiver functions derived from the extremely limited available earthquake data [*Shapiro et al.*, 2000; *Levin et al.*, 2002]. As for the teleseismic case, the force geometry and the source time function are assumed known. The amplitude and waveforms of the synthetics and the data are consistent to within the resolution of the method on the only non-nodal component, the transverse. The amplitude of the synthetic using the Kamchatkan crustal model varies by <1% from the observation and the synthetic based on the California model varies by only 5%. The major difference between the synthetics is a 3 s arrival time discrepancy, which is probably within the uncertainty in the reported origin time. Therefore, the Bezymianny landslide is consistent with the same μ_{app} as Mount St. Helens and Sheveluch.

5. Discussion

[17] In this paper we present direct measurements of friction in a large-scale natural setting. The seismic records analyzed here are consistent with μ_{app} = 0.2. From Equation 3, $0.6 \geq \mu \geq 0.2$ for three major volcanic landslides associated with eruptions.

[18] The most common current method of obtaining the dynamic friction of natural landslides is to use the mobility as a proxy for friction. The ratio of the altitude drop to runout length is equivalent to the coefficient of friction according to a rigid block energy balance [e.g., *Hsu*, 1975]. The mobility method has been criticized as inapplicable to deformable slides with internal dissipation and subject to geometric biases [*Iverson*, 1997; *Kilburn and Sorensen*, 1998]. Despite these problems, the lower bound of the actual friction as measured by the apparent friction μ_{app} = 0.2 overlaps with the values of 0.1–0.2 inferred from the mobility of these landslides [*Siebert*, 1984].

[19] The most striking result of this study is that all three landslides are consistent with the same apparent friction to within the resolution of the method. The uncertainty in translating μ_{app} to μ stems from unmodeled processes that generate a peak in the forces rather than a monotonic function (Figure 1). These unmodeled processes affect all the landslides in approximately the same way as all three exhibit the same source-time function. Therefore, the consistency in μ_{app} strongly suggests that all three landslides have the same μ, even though the value of μ can not be determined precisely for any individual event.

[20] The consistency of the apparent friction across all three landslides sheds some light on the hypothesis that hot gases from juvenile material reduce friction for volcanic landslides [*Voight et al.*, 1983]. The three landslides were vastly different in the relative quantities of hot gas available. Bezymianny had a directed blast with mass 50–100% that of its landslide, Mount St. Helens had a blast 20% as large as its landslide and Sheveluch had no directed blast [*Belousov*, 1995]. The consistency of apparent friction within measurement error despite variations in the amount of available hot gas suggests that volatiles from the magmatic system do not significantly reduce landslide friction.

6. Conclusions

[21] Acknowledging the limitations of this strictly forward-modeling study of historical records, we conclude that: (1) the seismic data is consistent with an apparent coefficient of friction of 0.2 for large volcanic landslides, (2) the actual areally averaged friction is between 0.2 and 0.6 and (3) volcanic gas in directed blasts does not affect the apparent friction and may not be a factor in lubricating landslides.

[22] **Acknowledgments.** The regional synthetic seismograms were calculated with programs written by L. Zhu. We thank A. Belousov and B. Voight for constructive reviews and R. Iverson for helpful discussions. The work was supported by NSF Grant EAR-0238455.

References

Belousov, A., Debris avalanche of the 1956 Bezymianny eruption, *Proc. of the Kagoshima Internat. Conf. on Volcanoes, Kagoshima, Japan*, 460–462, 1988.

Belousov, A., The Shiveluch volcanic eruption of 12 November, 1964; explosive eruption provoked by failure of the edifice, *J. Volcanol. Geotherm. Res.*, *66*, 347–365, 1995.

Belousov, A., Deposits of the 30 March 1956 directed blast at Bezymianny volcano, Kamchatka, Russia, *Bull. Volc.*, *57*, 649–662, 1996.

Dahlen, F., Single-force representation of shallow landslide sources, *Bull. Seism. Soc. Am.*, *83*, 130–143, 1993.

Dreger, D., and D. Helmberger, Determination of source parameters at regional distances with three-component sparse network data, *J. Geophys. Res.*, *98*, 8107–8125, 1993.

Glicken, H., Rockslide-debris avalanche of the May 18, 1980, Mount St. Helens Volcano, Washington, *U.S. Geol. Surv. Open-file Rep., 96-677*, 1996.

Hasegawa, H., and H. Kanamori, Source mechanism of the Magnitude 7.2 Grand Banks Earthquake of November 1929, *Bull. Seism. Soc. Am.*, *77*, 1984–2004, 1987.

Hsu, K., On sturzstroms—catastrophic debris streams generated by rockfalls, *GSA Bull.*, *86*, 129–140, 1975.

Iverson, R. M., The physics of debris flows, *Rev. Geophys.*, *35*, 245–296, 1997.

Julian, B., A. Miller, and G. Foulger, Non-double-couple earthquakes 1. theory, *Rev. Geophys.*, *36*(4), 525–549, 1998.

Kanamori, H., Mantle beneath the Japanese arc, *Phys. Earth Planet. Interiors*, *3*, 475–483, 1970.

Kanamori, H., and J. W. Given, Analysis of long-period seismic waves excited by the May 18, 1980, eruption of Mount St. Helens - a terrestrial monopole?, *J. Geophys. Res.*, *87*, 5422–5432, 1982.

Kanamori, H., J. W. Given, and T. Lay, Analysis of seismic body waves excited by the Mount St. Helens eruption of May 18, 1980, *J. Geophys. Res.*, *89*, 1856–1866, 1984.

Kawakatsu, H., Centroid single force inversion of seismic-waves generated by landslides, *J. Geophys. Res.*, *94*(B9), 12,363–12,374, 1994.

Kilburn, C., and S.-A. Sorensen, Runout lengths of sturzstroms: The control of initial conditions and of fragment dynamics, *J. Geophys. Res.*, *103*(B8), 17,877–17,884, 1998.

Levin, V., J. Park, M. Brandon, et al., Crust and upper mantle of Kamchatka from teleseismic receiver functions, *Tectonophysics*, *358*, 233–265, 2002.

Passechnik, I., Seismic and air waves which arose during an eruption of the volcano Bezymianny, on March 30, 1956, *Bull. Acad. Aci. USSR Geophys. Ser., Engl. Trans.*, 650–653, 1958.

Press, F., Earth models consistent with geophysical data, *Phys. Earth Planet. Interiors*, *3*, 3–22, 1970.

Shapiro, N., A. Gorbatov, E. Gordeev, et al., Average shear-wave velocity structure of the Kamchatka peninsula from the dispersion of surface waves, *Earth Planets Space*, *82*, 573–577, 2000.

Siebert, L., Large volcanic debris avalanches: Characteristics of source areas, deposits, and associated eruptions, *J. Volcanol. Geotherm. Res.*, *22*, 163–197, 1984.

Voight, B., Time scale for the first moments of the May 18 eruption, *U.S. Geol. Surv. Prof. Pap., 1250*, 69–86, 1981.

Voight, B., R. J. Janda, H. Glicken, et al., Time scale for the first moments of the May 18 eruption, *Geotechnique*, *33*, 243–273, 1983.

Zhu, L., and L. Rivera, A note on the dynamic and static displacements from a point source in multilayered media, *Geophys. J. Int.*, *148*, 619–627, 2002.

E. E. Brodsky, Department of Earth and Space Sciences, University of California, Los Angeles, CA, USA. (brodsky@ess.ucla.edu)

E. Gordeev, Geophys. Survey of Russ. Acad. of Sci., Petropavlovsk-Kamchatsky, Russia.

H. Kanamori, Seismo Lab, Caltech, Pasadena, CA, USA.